



# Mobius3D

# THE COMPLETE PATIENT QA SYSTEM



**3D PATIENT  
PLAN QA**



**3D IMRT/VMAT  
PRE TREATMENT QA**



**3D *IN VIVO*  
DAILY TREATMENT  
QA**



**ONLINE PATIENT  
POSITIONING QA**

**Upgrade your patient safety by bridging the gap between patient QA and machine QA:**

DoseLab, the complete TG-142 solution, is now integrated into Mobius3D!

Visit [mobiusmed.com/mobius3d](http://mobiusmed.com/mobius3d) to learn more or register for a bi-weekly webinar at [mobiusmed.com/webinars](http://mobiusmed.com/webinars)



**MOBIUS**  
MEDICAL SYSTEMS  
INNOVATIVE SOFTWARE FOR MODERN RADIATION ONCOLOGY

# Development of the open-source dose calculation and optimization toolkit matRad

Hans-Peter Wieser<sup>a)</sup>

*Department of Medical Physics in Radiation Oncology, German Cancer Research Center-DKFZ, Im Neuenheimer Feld 280, D-69120, Heidelberg, Germany*

Eduardo Cisternas, Niklas Wahl, Silke Ulrich, Alexander Stadler, Henning Mescher, Lucas-Raphael Müller, Thomas Klinge, Hubert Gabrys, and Lucas Burigo

*Department of Medical Physics in Radiation Oncology, German Cancer Research Center-DKFZ, Im Neuenheimer Feld 280, D-69120, Heidelberg, Germany*

*Department of Medical Physics in Radiation Oncology, Heidelberg Institute for Radiation Oncology-HIRO, Im Neuenheimer Feld 280, D-69120, Heidelberg, Germany*

Andrea Mairani, Swantje Ecker, Benjamin Ackermann, and Malte Ellerbrock

*Department of Medical Physics in Radiation Oncology, Heidelberg Ion Beam Therapy Center-HIT, Im Neuenheimer Feld 450, D-69120, Heidelberg, Germany*

*Department of Medical Physics in Radiation Oncology, Heidelberg Institute for Radiation Oncology-HIRO, Im Neuenheimer Feld 280, D-69120, Heidelberg, Germany*

Katia Parodi

*Department of Medical Physics in Radiation Oncology, Ludwig-Maximilians-Universität München, Am Coulombwall 1, D-85748, Garching, Germany*

*Department of Medical Physics in Radiation Oncology, Heidelberg Ion Beam Therapy Center-HIT, Im Neuenheimer Feld 450, D-69120, Heidelberg, Germany*

*Department of Medical Physics in Radiation Oncology, Heidelberg Institute for Radiation Oncology-HIRO, Im Neuenheimer Feld 280, D-69120, Heidelberg, Germany*

Oliver Jäkel

*Department of Medical Physics in Radiation Oncology, German Cancer Research Center-DKFZ, Im Neuenheimer Feld 280, D-69120, Heidelberg, Germany*

*Department of Medical Physics in Radiation Oncology, Heidelberg Ion Beam Therapy Center-HIT, Im Neuenheimer Feld 450, D-69120, Heidelberg, Germany*

*Department of Medical Physics in Radiation Oncology, Heidelberg Institute for Radiation Oncology-HIRO, Im Neuenheimer Feld 280, D-69120, Heidelberg, Germany*

Mark Bangert

*Department of Medical Physics in Radiation Oncology, German Cancer Research Center-DKFZ, Im Neuenheimer Feld 280, D-69120, Heidelberg, Germany*

*Department of Medical Physics in Radiation Oncology, Heidelberg Institute for Radiation Oncology-HIRO, Im Neuenheimer Feld 280, D-69120, Heidelberg, Germany*

(Received 14 December 2016; revised 15 March 2017; accepted for publication 17 March 2017; published xx xxxx xxxx)

**Purpose:** We report on the development of the open-source cross-platform radiation treatment planning toolkit matRad and its comparison against validated treatment planning systems. The toolkit enables three-dimensional intensity-modulated radiation therapy treatment planning for photons, scanned protons and scanned carbon ions.

**Methods:** matRad is entirely written in Matlab and is freely available online. It re-implements well-established algorithms employing a modular and sequential software design to model the entire treatment planning workflow. It comprises core functionalities to import DICOM data, to calculate and optimize dose as well as a graphical user interface for visualization. matRad dose calculation algorithms (for carbon ions this also includes the computation of the relative biological effect) are compared against dose calculation results originating from clinically approved treatment planning systems.

**Results:** We observe three-dimensional  $\gamma$ -analysis pass rates  $\geq 99.67\%$  for all three radiation modalities utilizing a distance to agreement of 2 mm and a dose difference criterion of 2%. The computational efficiency of matRad is evaluated in a treatment planning study considering three different treatment scenarios for every radiation modality. For photons, we measure total run times of 145 s–1260 s for dose calculation and fluence optimization combined considering 4–72 beam orientations and 2608–13597 beamlets. For charged particles, we measure total run times of 63 s–993 s for dose calculation and fluence optimization combined considering 9963–45574 pencil beams. Using a CT and dose grid resolution of 0.3 cm<sup>3</sup> requires a memory consumption of 1.59 GB–9.07 GB and 0.29 GB–17.94 GB for photons and charged particles, respectively.

**Conclusion:** The dosimetric accuracy, computational performance and open-source character of matRad encourages a future application of matRad for both educational and research purposes. © 2017 The Authors. *Medical Physics* published by Wiley Periodicals, Inc. on behalf of American Association of Physicists in Medicine. [<https://doi.org/10.1002/mp.12251>]

Key words: DICOM, dose calculation, inverse planning, optimization, radiation therapy

## 1. INTRODUCTION

Science relies on evidence. Hypotheses have to be tested and verified — preferably by different research groups and methodologies — in order to be accepted, improved, or rejected. However, also in the context of software, reproducing evidence becomes more difficult as the ever increasing complexity of computer programs can barely be described by a research paper alone. Ideally, the source code is released alongside publications to facilitate scientific advancement.<sup>1</sup>

An increased importance of more and more complex computer programs can also be observed in the field of radiation therapy (RT) treatment planning. Here, mostly commercial companies provide software to cover the various needs in the clinic and beyond. Due to the high safety requirements of medical applications, commercial software is usually available in closed software architecture which compromises a flexible usage, e.g., for educational purposes and research. Consequently, some research groups (a) maintain custom-tailored treatment planning solutions,<sup>2–4</sup> (b) make extensive use of scripting interfaces of clinical treatment planning systems to build a bridge between flexible custom code and closed architectures, or (c) collaborate directly with vendors to get deeper access to the code of the treatment planning system.

Various open-source software projects such as FoCa,<sup>5</sup> PPlanUNC,<sup>6</sup> CERR,<sup>7</sup> REGGUI\* and SlicerRT<sup>8</sup> including the proton dose engine from Ref. 9 already address the limited accessibility of flexible software solutions in radiation oncology. However, most of the current open-source solutions focus on specific radiation treatment planning steps such as image processing and plan analysis and/or dose calculation and optimization is limited to a single radiation modality. Here, we describe the development of matRad, an open-source multimodality dose calculation and optimization toolkit for radiation treatment planning along with a comparison against validated treatment planning systems (TPS). matRad is published under the GNU public licence in the hope that it will be useful, but without any warranty<sup>†</sup>. The software is entirely written in the numerical computation environment Matlab<sup>‡,10</sup> and supports intensity-modulated radiation therapy treatment planning for photons, scanned protons, and scanned carbon ions at clinically adequate resolution. matRad provides a high degree of accessibility and

flexibility for both research and educational purposes. The software package is hosted on the web-based code versioning service GitHub<sup>§</sup> and comprises, besides the source code itself, anonymized open-source patient data, as well as physical and biological base data.

This contribution is not a classical research paper addressing a single scientific question. Instead, it is rather an in-depth scientific description of matRad and its underlying algorithms. Modules and core functionalities of matRad are described in section 2. The comparison of the dose engine (including three-dimensional calculations of the relative biological effect for carbon ions) against clinically approved treatment planning platforms, the evaluation of the fluence optimization engine, and a detailed analysis of the computational efficiency are presented in section 3. Sections 4 and 5 discuss and conclude the paper.

## 2. MATERIAL AND METHODS

Sections 2.A and 2.B describe the base and patient data that are supplied as part of the matRad release; sections 2.C–2.H explain the software design and core functionalities of matRad. Throughout this paper, lower case emphasized abbreviations (e.g., *pln*, *ct*, etc.) directly refer to variable names as used in matRad to make it easier for the reader to directly relate to the code.

### 2.A. Base data

The matRad source code includes base data modeling generic radiation devices for photons, protons, and carbon ions. Base data for every radiation modality are stored as a single file in Matlab's native file format and loaded dynamically into matRad depending on the current treatment planning scenario.

*a. Photons:* Base data for the photon dose calculation algorithm are obtained from the clinically approved photon dose calculation engine PDC++<sup>11</sup> and describes the decomposed lateral scattering kernels and depth dose components as detailed in Ref. 12 for a 6 MV linear accelerator for multiple source to surface distances (SSDs).

*b. Protons:* Analytical calculations according to Ref. 13 are used to approximate integrated proton depth dose profiles in water for 114 proton beam energies ranging from 31.72 MeV to 236.1 MeV which correspond to peak positions from 7 mm to 347 mm. Lateral beam broadening of the proton beam due to multiple Coulomb scattering is calculated as proposed by Ref. 14 and added quadratically to the initial beam widths

\*<https://www.openreggui.org/>

<sup>†</sup>The complete matRad license agreement is available at <https://github.com/e0404/matRad/blob/master/LICENSES.txt>.

<sup>‡</sup>We actively test compatibility with Matlab versions  $\geq 8.3$  (R2014a)

<sup>§</sup><http://www.matrad.org>

taken from Ref. 15. Additional widening of the initial beam width in air is not considered. If corresponding look up tables are provided as part of the base data, the beam widening effect in air is automatically considered. For a detailed description of the beam model we refer to Ref. 16. Both, depth dose profiles and the lateral beam properties are stored for each initial beam energy as a function of depth in water.

*c. Carbon ions:* Integrated carbon ion depth dose profiles are based on FLUKA Monte Carlo simulations describing interactions of carbon ions and their fragments with a generic beam line considering a ripple filter of 3 mm. Monte Carlo simulations were performed in water similar to Ref. 16. In total, 121 carbon ion depth dose profiles linearly spaced from 115.23 MeV to 398.84 MeV depicting peak positions from 32 mm to 294 mm are part of the carbon ion base data file. Lateral beam spread in water was calculated in line with Ref. 16 considering a correction term for heavy ions. To enable biological treatment planning, each mono-energetic carbon ion depth dose profile is complemented by dose-averaged  $\bar{\alpha}$ - [ $\text{Gy}^{-1}$ ] and  $\bar{\beta}$ - [ $\text{Gy}^{-2}$ ] profiles as a function of depth in water describing the biological beam properties according to the linear quadratic model (LQM).<sup>17</sup> The biological base data were obtained from the 4th version of the local effect model (LEM IV).<sup>18</sup> Biological effects for multiple particles were computed following the approach taken in Ref. 19. Consequently, the validity of the biological base data is limited to therapeutical doses smaller than 10 Gy(RBE). For the calculation of dose-averaged  $\bar{\alpha}$ - and  $\bar{\beta}$ -profiles, it was necessary to account for synergetic effects originating from mixed radiation fields by the application of a beam mixing model according to Ref. 20. Two biological base datasets characterizing an early and late responding tissue were generated with LEM IV from reference photon LQM parameters of ( $\alpha = 0.1 \text{ Gy}^{-1}$ ,  $\beta = 0.05 \text{ Gy}^{-2}$ ) and ( $\alpha = 0.5 \text{ Gy}^{-1}$ ,  $\beta = 0.05 \text{ Gy}^{-2}$ ), hence  $\frac{\bar{\alpha}}{\bar{\beta}}$  ratios are 2 Gy and 10 Gy, respectively.

Integrated depth dose curves for protons and carbon ions are given in  $\text{MeV cm}^2 \text{ g}^{-1}$  and converted within the particle dose calculation to  $\text{Gy mm}^2$  per million primaries [1e6]. Given that the lateral components of the dose calculation exhibit the unit  $\text{mm}^2$ , the weight of the pencil beam directly corresponds to the number of particles [1e6] while the dose is given in Gy.

The software design allows for a straightforward incorporation of additional custom base data, e.g., to simulate additional particle species or alternative beam lines. Multiple base datasets describing different beam lines can be kept in parallel.

## 2.B. Patient data

The matRad software toolkit comes with five anonymized open-source patient/phantom datasets for treatment planning which are stored in a custom Matlab file format (\*.mat). Besides a cubic box phantom, four additional cases (prostate, liver, head and neck, and TG119 phantom) stemming from the common optimization for radiation therapy (CORT) dataset,<sup>21</sup> are included into the public code base. The CORT dataset is an open-source dataset intended to be used by researchers when developing and benchmarking radiation

treatment planning algorithms. Each dataset contains computed tomography (CT) images (*ct*) as well as segmentations and predefined treatment planning parameters (*cst*).

## 2.C. Interfaces

matRad features a DICOM (Digital Imaging and Communications in Medicine) import module allowing for the conversion of DICOM data (CT and RT structure set) into matRad's custom patient data format (*ct,cst*). Consequently, patient data need only to be converted once. matRad's DICOM import functionality requires the image processing toolbox of Matlab as we rely on built-in functions to import DICOM data. Aside from that no other toolbox is needed to run matRad. The DICOM import can either be started via the graphical user interface (GUI) or by calling the corresponding function manually.

During the DICOM import, the grid resolution for the resulting CT cube (*ct*) can be adapted. By default, the original CT resolution is used, adaption of the resolution uses trilinear interpolation. The resolution of the CT cube automatically defines the dose grid resolution used later on for dose calculation and optimization. Currently, matRad is not able to compute dose on a different grid than the resolution of the interpolated CT cube. However, if a DICOM RT dose volume is imported along with a CT, it is possible to use the original resolution of the dose volume; the CT cube will be interpolated accordingly.

In order to accurately account for tissue heterogeneities during radiotherapy treatment planning, Hounsfield units of the CT scans are linked to electron densities (photons) or relative stopping powers in water (particles) by means of Hounsfield lookup tables (HLUT). If no HLUT is provided, a default lookup table is used instead.

matRad also supports the import of DICOM RT dose and RT plan objects. However, the plan import has only been tested for our own setup, i.e., a Siemens Artiste<sup>TM</sup> linear accelerator including the Siemens 160 MLC<sup>TM</sup> in combination with Raystation and for scanning beam lines at the Heidelberg Ion-Beam Therapy Center in combination with Syngo RT Planning. Furthermore, \*.nrrd files corresponding to either CT datasets, binary RT structure masks and/or dose volumes can be imported with the binary file importer. Complementary, to the import module is an export module which is capable of exporting CT, dose volumes as well as binary segmentations to the \*.vtk, \*.nrrd and \*.mha file format.

## 2.D. Workflow

matRad models the radiation therapy treatment planning workflow by sequential function calls which can either be triggered using Matlab's command line prompt or matRad's GUI (see 2.H).

The first step of the workflow is to load patient data consisting of a CT dataset (*ct*) and segmentations (*cst*). Loading data can either be achieved via the DICOM or binary import interface (see 2.C) or by directly importing patient data stored

in matRad's custom format. Next, treatment plan parameters are specified within a Matlab structure (*pln*) to determine the radiation modality, beam angles, and number of fractions, among others. Afterwards, the beam geometry (*stf*) describing the placement of bixels/beamlets for photons or the individual pristine pencil beams for charged particles is generated (see 2.E). Once the beam geometry is defined, the dose calculation function (see 2.F) can be called returning a dose influence structure (*dij*) holding the dose contribution from each bixel/pencil beam. Then photon and charged particle fluence distributions can be optimized according to user-defined objectives and constraints (see 2.G). In the case of treatment planning for photons, a multileaf collimator (MLC) sequencing algorithm can be applied to translate continuously optimized fluences into deliverable segments. Moreover, we provide an experimental direct aperture optimization implementation. Resulting dose distributions are saved in the variable *resultGUI* and can be analyzed in the GUI (see 2.H) which also supports DVH computation and additional dose statistics. Reoptimization using different optimization parameters (penalties, objectives, constraints) can be repeated until the dose distribution is deemed satisfying.

## 2.E. DEFINITION OF IRRADIATION GEOMETRY

matRad uses the LPS (Left, Posterior, Superior) coordinate system<sup>||</sup>. While matRad's dose calculation covers all segmented structures by default, the primary fluence considered for optimization is restricted to the projection of the target onto the beam's eye view for every beam orientation. We use an approach similar to Ref. 22. Therefore, the patient geometry is transferred beam-wise into the beam's eye view coordinate system and the target volume is projected onto the iso-center plane which is perpendicular to the connection of the virtual radiation source and the iso-center<sup>¶</sup>. Next, equidistant rays are selected to cover the entire target volume (the lateral spacing can be controlled via the parameter *pln.bixelWidth*). In case of photons, each ray corresponds to a discrete rectangular fluence element, i.e., one bixel. In case of particles, pencil beams are additionally placed longitudinally on the ray to also cover the target volume in depth. The irradiation geometry or beam steering information is stored in a separate Matlab struct called *stf*.

## 2.F. Dose calculation

The core of the dose calculation engine is comprised of two nested *for* loops where the outer loop runs over the number of beams and the inner loop processes all rays from the current beam. For charged particles, there is an additional inner loop responsible for calculating the dose deposition of multiple pencil beams per ray.<sup>¶</sup> matRad performs an exact

calculation of the radiological depth for the entire irradiated volume using a ray tracing algorithm as described previously.<sup>11,23</sup> Geometrical distances from the virtual radiation source and lateral distances to the central ray are computed by standard matrix vector algebra. For optimization, matRad uses the dose influence matrix concept where the dose  $d_i$  in voxel  $i$  can be computed with a matrix vector product according to

$$d_i = \sum_j D_{ij} w_j \quad \text{or:} \quad \vec{d} = D \vec{w}. \quad (1)$$

Here, the matrix  $D$  stores the dose contribution to voxel  $i$  from bixel/pencil beam  $j$  at unit intensity and  $w_j$  corresponds to the weight of bixel/pencil beam  $j$ . The dose influence matrix  $D$  is stored with Matlab's built-in double precision sparse matrix format. If fluence optimization is not required, it is possible to bypass the storing of the matrix  $D$  for both photons and charged particles. For photons, there is additional functionality implemented that allows for direct dose calculation based on aperture shapes and weights obtained via a DICOM RT plan import. Filling the sparse matrix column block-wise ensures efficient filling times. The dose influence matrix is stored in a variable named *dij* which is then used in the subsequent fluence optimization.

*d. Photons* matRad facilitates a singular value decomposed pencil beam algorithm to calculate photon dose deposition.<sup>12</sup> The decomposition of pencil beam kernels into three components reduces the number of two-dimensional convolutions to three without compromising the dosimetric accuracy. As a consequence, the calculation time compared to other pencil beam algorithms can be minimized. The pencil beam kernels, which account for dose contributions stemming from primary and scattered radiation, are precomputed for multiple SSDs. To reduce the memory requirements of the dose influence matrix used for optimization, matRad facilitates importance sampling as introduced by Ref.24.

*e. Charged Particles* matRad assumes an active spot scanning dose application and features the conventional dose-to-water-pencil beam algorithm according to the work of Ref. 25. Dose deposition is calculated for each pencil beam individually and is defined as the product of a depth component and a two-dimensional lateral component. The lateral rotationally symmetric beam profile is modeled by a single Gaussian or a weighted superposition of two Gaussian components<sup>16</sup> to account for the low-dose halo more accurately<sup>\*\*</sup>. The actual code for the physical dose calculation for both, protons and carbon ions is the same. For biological optimization in carbon ion treatment planning, two additional sparse matrices are computed during the calculation of dose influence data. Taking into account the radiological depth,

<sup>||</sup>See <https://github.com/e0404/matRad/wiki/The-matRad-coordinate-system> for a detailed illustration.

<sup>¶</sup>See <https://github.com/e0404/matRad/wiki/Dose%20influence-matrix-calculation#ray-and-bixel-concept> for a detailed illustration.

<sup>\*\*</sup>Note that the open-source release of matRad does not include base data for particle dose calculation relying on a lateral beam model using two Gaussian components. While we use such data to accurately model the beam lines at the Heidelberg Ion-Beam Therapy Center for the comparison as detailed in sections 3.A.2 and 3.A.3, we are not able to share this base data.

TABLE I. Supported objective and constraint functions by matRad with dose  $d_i$  in voxel  $i$ , prescribed dose  $\hat{d}$ , dose  $\tilde{d}$  at prescribed volume, structure  $S$ , number of voxels in structure  $N_S$ , equivalent uniform dose (EUD) exponent  $a$ , Heaviside function  $\Theta(x)$ , and log-sum-exp function parameter  $\kappa = 10^{-3}$ . Min/max mean and min/max EUD constraints are not explicitly stated but are supported by matRad.

Objectives		Constraints	
$f_{sq\ deviation}$	$= \frac{1}{N_S} \sum_{i \in S} (d_i - \hat{d})^2$		
$f_{sq\ under\ dosage}$	$= \frac{1}{N_S} \sum_{i \in S} \Theta(\hat{d} - d_i) (d_i - \hat{d})^2$	$c_{min\ dose}$	$= d_{min} - \kappa \log(\sum_{i \in S} e^{\frac{d_{min} - d_i}{\kappa}})$
$f_{sq\ over\ dosage}$	$= \frac{1}{N_S} \sum_{i \in S} \Theta(d_i - \hat{d}) (d_i - \hat{d})^2$	$c_{max\ dose}$	$= d_{max} + \kappa \log(\sum_{i \in S} e^{\frac{d_i - d_{max}}{\kappa}})$
$f_{mean}$	$= \frac{1}{N_S} \sum_{i \in S} d_i$	$c_{mean}$	$= \frac{1}{N_S} \sum_{i \in S} d_i$
$f_{EUD}$	$= (\frac{1}{N_S} \sum_{i \in S} d_i^a)^{\frac{1}{a}}$	$c_{EUD}$	$= (\frac{1}{N_S} \sum_{i \in S} d_i^a)^{\frac{1}{a}}$
$f_{min\ DVH}$	$= \frac{1}{N_S} \sum_{i \in S} \Theta(\hat{d} - d_i) \Theta(d_i - \tilde{d}) (d_i - \hat{d})^2$	$c_{min\ DVH}$	$= \frac{1}{N_S} \sum_{i \in S} \Theta(\tilde{d} - d_i)$
$f_{max\ DVH}$	$= \frac{1}{N_S} \sum_{i \in S} \Theta(d_i - \hat{d}) \Theta(\tilde{d} - d_i) (d_i - \hat{d})^2$	$c_{max\ DVH}$	$= \frac{1}{N_S} \sum_{i \in S} \Theta(d_i - \hat{d})$

dose averaged  $\bar{\alpha}$  and  $\sqrt{\beta}$  values are linearly interpolated and multiplied with the corresponding physical dose.<sup>30</sup> The resulting quantities are stored in alpha dose and square root beta dose sparse matrices.

## 2.G. Optimization

matRad determines the optimal radiation fluence through minimization of a weighted sum of objective functions that can be subject to additional constraints:

$$\min_{w \in \mathbb{R}^B} f(w) = \sum_n p_n f_n(w) \quad (2)$$

$$\text{subject to } c_k^l \leq c_k(w) \leq c_k^u \\ 0 \leq w$$

Here,  $f(w)$  denotes the overall objective function which is composed by individual components  $f_n(w)$  with relative weighting (also often referred to as penalty)  $p_n$ .  $c_k^l$  and  $c_k^u$  indicate lower and upper bounds on the  $k$ -th constraint function  $c_k(w)$ . The positivity constraint  $0 \leq w$  ensures that only positive radiation fluences are considered.

matRad relies on the interior point optimizer package (IPOPT)<sup>26</sup> to solve the fluence optimization problem defined in Eq. (2). IPOPT is made available by the COIN-OR<sup>††</sup> initiative and is a free software package for large-scale nonlinear constrained optimization problems. Originally, IPOPT was written in Fortran and C, but meanwhile also a C++ version is available including a Matlab interface based on Matlab EXecutable files (\*.MEX), which allows to call C++ files within the Matlab environment.

matRad provides callback functions that are passed on to IPOPT to evaluate objectives as well as constraints and to retrieve information about the gradient of the objective function as well as the jacobian of the constraint functions. Furthermore, IPOPT requires a set of initial bixel/pencil beam weights  $w$  and an options file. Among others, the latter allows to define convergence criteria (e.g., maximum number of iterations and acceptable convergence tolerance).

<sup>††</sup>Computational infrastructure for operations research, <http://coin-or.org>

The exact definition of the composition of  $f(w)$  including constraints  $c_k$  is up to the user. Multiple objectives and constraints can be defined and weighted for each structure individually in the *cst* variable or via a table in the GUI. Supported objective functions and constraints for physical and biological optimization are shown in Table I.

For treatment planning with photons, we perform a fluence-based optimization of the physical dose by default. To translate the resulting continuous fluence profiles into deliverable MLC segments, matRad features MLC sequencing algorithms of Refs. 27,28,39. Moreover, matRad includes an experimental direct aperture optimization module following the work of Ref. 29. For protons, it is possible to factor in a constant relative biological effectiveness (RBE) of 1.1 by activating biological optimization. For carbon ions, biological optimization is supported in two different flavors: it is possible to optimize (a) the biological effect according to Ref. 30 or (b) the RBE-weighted dose according to Ref. 31.

## 2.H. Graphical user interface — GUI

matRad provides a GUI that allows to visualize and explore the CT and superimposed transparent dose distribution (see Fig. 1). Furthermore, the sequential treatment planning workflow can be triggered from the GUI. Data elements of the GUI are automatically synced with Matlab's base workspace and vice versa. By this means, a flexible data manipulation environment for algorithm development is ensured as the user can switch between the command line interface and the GUI at any time while always working with consistent data.

## 2.I. Availability

The complete source code including beam and patient data is hosted on the web-based repository service GitHub and can either be downloaded as zip and tar ball or can be cloned with a version control system supporting Git. To support new matRad users, we provide a quick set up guide and a technical documentation in the form of a Wiki. The Github framework allows everyone to contribute to a transparent, moderated code development process with clear authorship tracking.

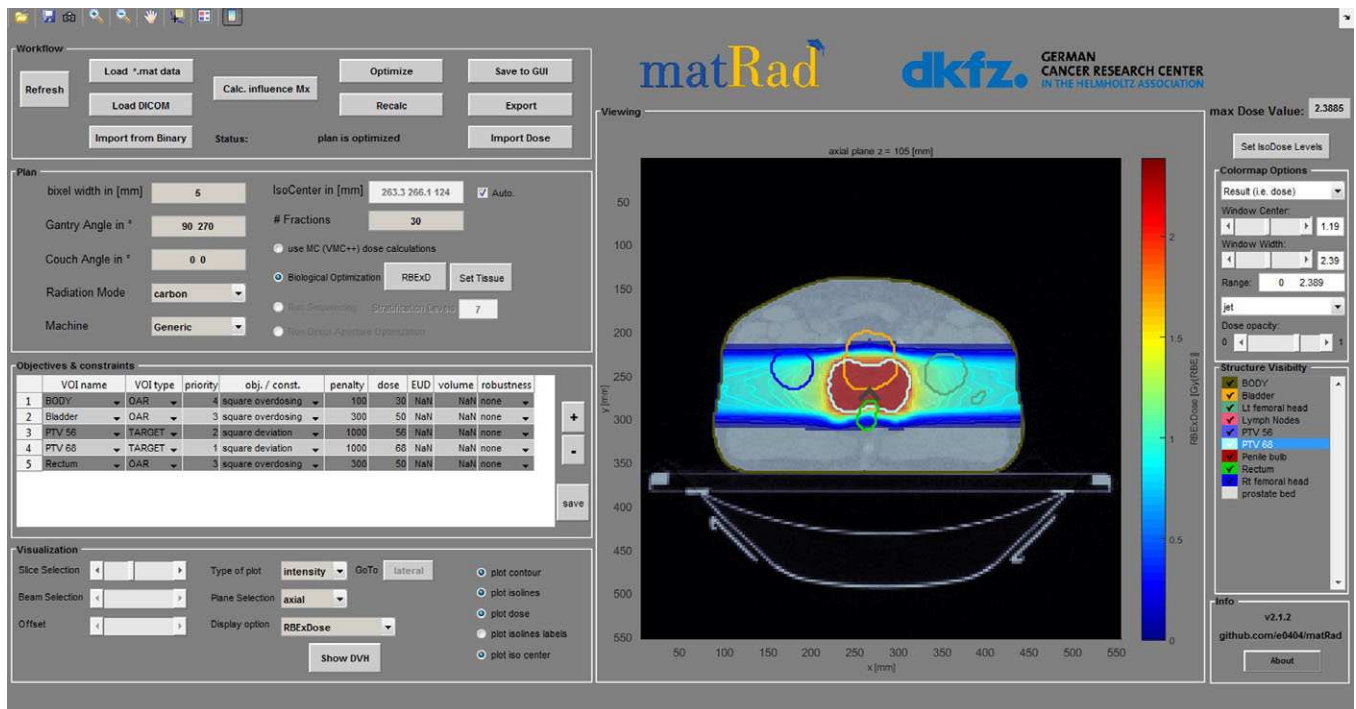


FIG. 1. The graphical user interface of matRad is grouped into several functional blocks, whereas each block addresses certain aspects of treatment planning (e.g., plan definition, data exploration, defining objectives and constraints for optimization, etc.)

### 3. RESULTS

#### 3.A. Comparison of dose calculation

To compare matRad's dose calculation, fluence optimization and dose calculation were done on a clinically approved reference platform and then dose distributions were recalculated in matRad. Section 3.A.1 describes the comparison of the photon dose calculation engine and sections 3.A.2 and 3.A.3 describe the comparison of the particle dose engines for protons and carbon ions separately. Three-dimensional  $\gamma$ -analysis, according to Ref 32, was employed in each case using a distance to agreement (dta) of 2 mm and a dose difference ( $\Delta d$ ) criterion of 2%. Whereupon only dose points exceeding 2% of the maximal dose value are considered for the  $\gamma$ -analysis. The results presented in this chapter are based on matRad version 2.2.0.

##### 3.A.1. Photons

Inverse treatment planning for a cranial case was performed with the clinically approved in-house photon dose calculation module PDC++<sup>11</sup> in combination with the inverse planning system KonRad.<sup>22</sup> The intensity-modulated radiation treatment plan comprised seven coplanar beams with gantry angles 0°, 52°, 103°, 154°, 206°, 257°, and 309°. Corresponding couch angles were set to 0°. The resulting DICOM RT plan holding information about the MLC shapes was imported together with the optimized dose distribution into matRad. Then, the photon dose distribution was recalculated in matRad and compared against the reference dose distribution (see Fig. 2). The CT cube and the dose distribution

exhibited the same dimensions ( $512 \times 512 \times 104$ ) and the same spatial resolution ( $x = 0.781 \text{ mm}$ ,  $y = 0.781 \text{ mm}$ ,  $z = 3 \text{ mm}$ ).

CT slices in Figs. 2(a) and 2(b) are overlaid by isodose lines and transparent dose colorwash. Figure 2(c) illustrates the absolute difference of the dose distributions shown in Figs. 2(a) and 2(b). Although isolated voxels close to the skin surface exhibit dose differences of up to 0.22 Gy, i.e., a relative deviation of 12% of the prescribed fraction dose of 1.8 Gy, dose differences in the inner part of the head and especially within the planning target volume (PTV) are by factor 6 smaller. The maximum dose difference within the PTV of the shown iso-center slices is 0.035 Gy (see Fig. 2(c)). The three-dimensional  $\gamma$ -analysis, shown in Fig. 2(d), applies a distance to agreement of 2 mm and a dose-difference criterion of 2% resulting in a global pass rate of 99.82%.

The dosimetric differences between matRad and PDC++ can be explained by discretization effects of the underlying ray tracing. Due to the pronounced dose build-up upon entering the patient, small differences in the calculated radiological depth may result in isolated cases to substantial deviations in dose. However, 90% of voxels lying 3 cm deep in the patient exhibit a dose difference below 0.0135 Gy, i.e., 0.75% of the prescribed dose.

##### 3.A.2. Protons

matRad's particle dose engine for protons is compared against the treatment planning system Syngo RT Planning (Siemens, Erlangen, Germany) which is currently used at the Heidelberg Ion-Beam Therapy center (HIT). For

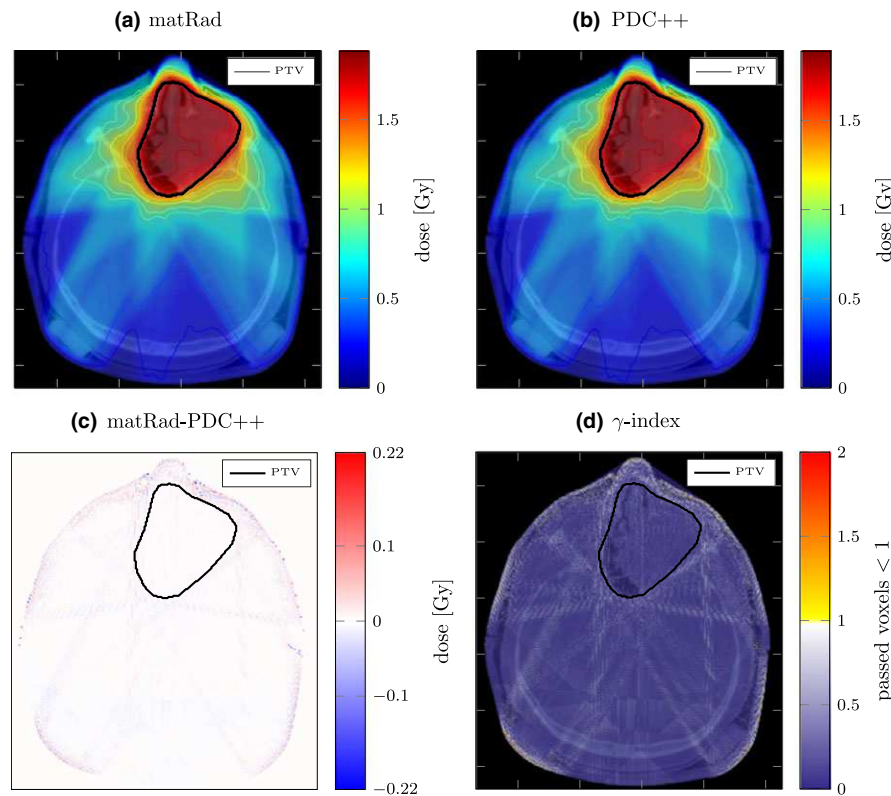


FIG. 2. Transversal slices of an intensity-modulated photon therapy treatment plan using seven beams with gantry angles of  $0^\circ$ ,  $52^\circ$ ,  $103^\circ$ ,  $154^\circ$ ,  $206^\circ$ ,  $257^\circ$ , and  $309^\circ$  — corresponding couch angles are  $0^\circ$ . The CT data overlaid with a transparent dose colorwash and isodose lines are shown in (a) and (b). (a) Dose distribution computed with matRad. (b) Dose distribution computed with PDC++. Their absolute difference is shown in (c) and the result of the  $\gamma$ -analysis ( $dta = 2$  mm,  $\Delta d 2\%$ ) is superimposed on the CT in (d). The global pass rate ( $\gamma \leq 1$ ) amounts to 99.82%.

protons, we compare the physical dose and not the RBE-weighted dose because the clinically applied constant RBE of 1.1 simply scales up the physical dose by 10%.

Three dose distributions depicting pristine proton beams with peak positions 5 cm, 15 cm, and 25 cm are considered and shown in Figs. 3(a) and 3(b). Central depth dose profiles are given in Fig. 3(a) for each pristine proton beam. We observe good agreement between matRad and the validated TPS Syngo RT Planning. The same holds true for the lateral dose profiles plotted for each beam at the peak position (see Fig. 3(b)). Profiles were scaled to spread them for visualization. As matRad employs the same double Gaussian lateral beam model as Syngo RT Planning, the lateral dose profiles also show reasonable agreement in the low dose region. Both, the matRad dose distribution and the reference dose distribution hold the same image dimensions ( $512 \times 512 \times 370$ ) and exhibit the same voxel resolution ( $x = 1$  mm,  $y = 1$  mm,  $z = 1$  mm). A global  $\gamma$ -analysis confirms good agreement with 100% pass rates for each evaluated pencil beam using  $\gamma$ -criteria of ( $dta = 2$  mm,  $\Delta d = 2\%$ ). We decided to plot profiles in the most sensitive regions, namely central profiles and lateral profiles at the peak position to reveal possible deviations in magnitude best. Showing either lateral or depth integrated dose profiles might obscure such deviations.

To evaluate the proton dose engine of matRad for a realistic treatment plan, a comparison of a cranial case is shown in Figs. 3(c)–3(e). Inverse treatment planning is done on the Syngo RT Planning platform using a constant RBE of 1.1. The resulting DICOM plan including pencil beam weights and dose distribution are imported into matRad in order to recalculate the dose. The CT image and dose distribution dimensions are ( $310 \times 310 \times 339$ ) possessing a voxel resolution of ( $x = 1$  mm,  $y = 1$  mm,  $z = 1$  mm).

As depicted in Fig. 3(c), matRad's dose calculation inside the PTV exhibits subtle spikes on the 2% level. We want to point out that this is not an artifact of our algorithm as we observe also a similar pattern for the Syngo RT Planning dose distribution. This behavior can be explained by the finite spacing of the Bragg peaks of the individual pencil beams in depth in combination with a coarser grid used during optimization. However, as the two jagged dose distributions from Syngo RT and matRad do not match perfectly, we also observe a jagged dose difference in Figs. 3(d) and 3(e). This phenomenon can be explained by the different resolutions used for the ray tracing. While Syngo RT Planning facilitates ray tracing on the original CT resolution, matRad relies on the CT interpolated at the  $1 \times 1 \times 1$  mm dose grid resulting in slight differences in the calculated depth for individual dose grid points.

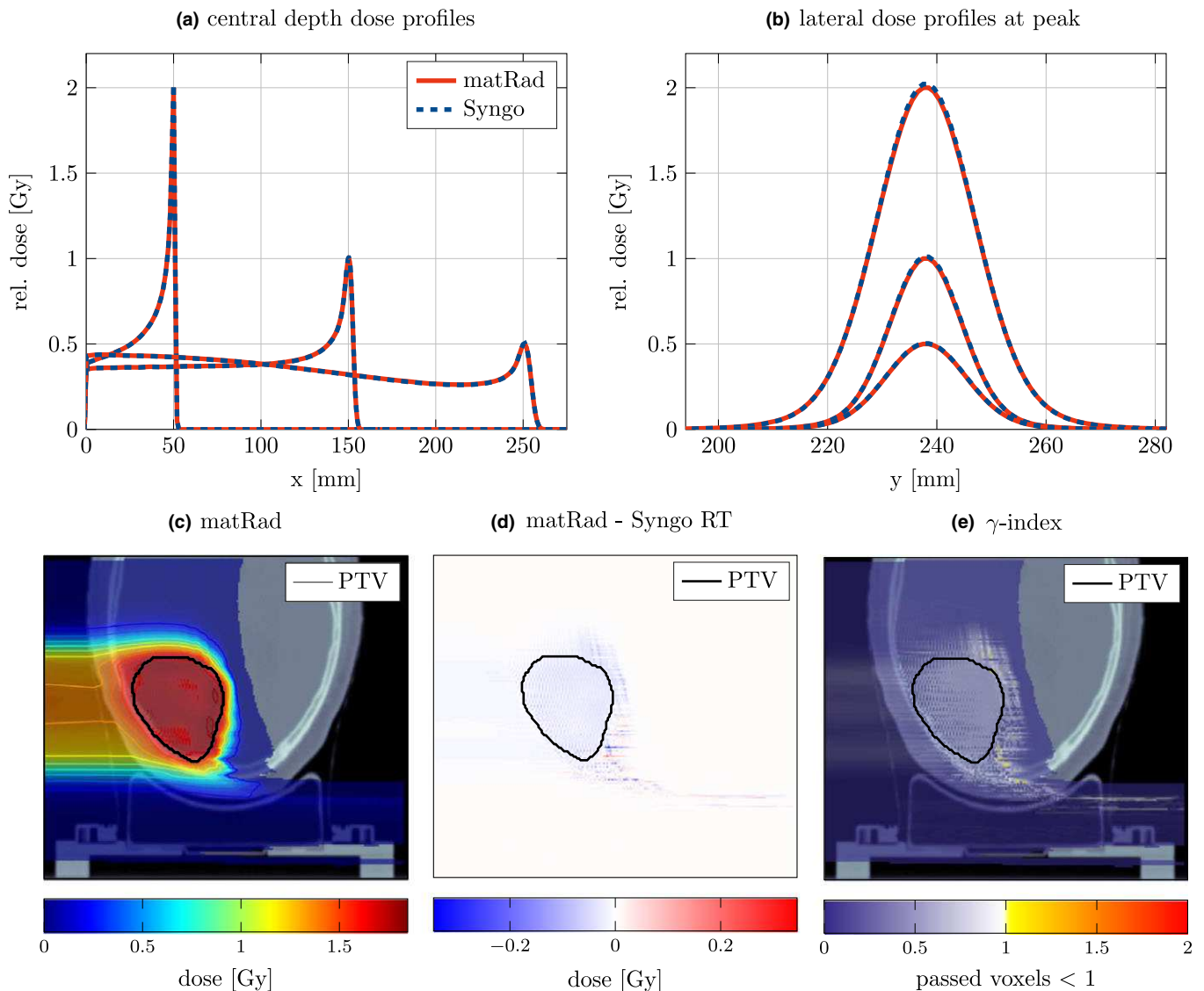


FIG. 3. Comparison of the proton dose calculation engine between Syngo RT Planning and matRad. Dashed lines in (a) and (b) refer to dose values calculated by Syngo RT whereas solid lines indicate dose values originating from matRad. Three pristine proton beams with peak positions at 5 cm, 15 cm, and 25 cm are evaluated. (a) Central physical dose profile of each beam as a function of depth. (b) Lateral physical dose profile at the peak positions. For a better separation of the data, profiles have been individually rescaled to maxima at 2, 1, and 0.5. (c)–(e) Transversal slices of an intensity-modulated proton therapy treatment plan for a cranial case using one beam with gantry angle  $270^\circ$  and couch angle  $0^\circ$ . (c) CT data superimposed with transparent dose colorwash and isodose lines calculated with matRad. The absolute difference between matRad and Syngo RT planning is shown in (d). The result of the  $\gamma$ -analysis is illustrated in (e). The global pass rate is 99.84%.

However, 90% of voxels receiving doses  $> 0$  deviate less than 0.025 Gy, i.e., 1.4% of the prescribed physical dose of 1.82 Gy. The  $\gamma$ -analysis shown in Fig. 3(e) results in a global pass rate of 99.84% using criteria of ( $d_{\text{ta}} = 2$  mm,  $\Delta d = 2\%$ ).

### 3.A.3. Carbon ions

The comparison of the particle dose engine for carbon ions is done in analogy to the comparison for protons. First, the physical and RBE-weighted dose depositions of three single energy carbon ion beams in a water phantom are calculated in matRad and compared separately against computations of the validated TPS Syngo RT Planning.

Second, the same cranial case used before for protons is planned with Syngo RT Planning for carbon ions and then recalculated in matRad.

We adapted the biological base data in matRad to rely on LEM I thereby ensuring consistency to the Syngo RT platform<sup>††</sup>. The RBE-weighted dose is calculated differently in Syngo and matRad. On the one hand, Syngo RT Planning features a Monte Carlo-based assessment of the relative biological effectiveness within the patient as initially reported in Ref. 31. Syngo RT Planning is configured to perform 1000 Monte Carlo loops to simulate the accumulated damage

<sup>††</sup>biological base data originating from LEM I is not part of the public code base

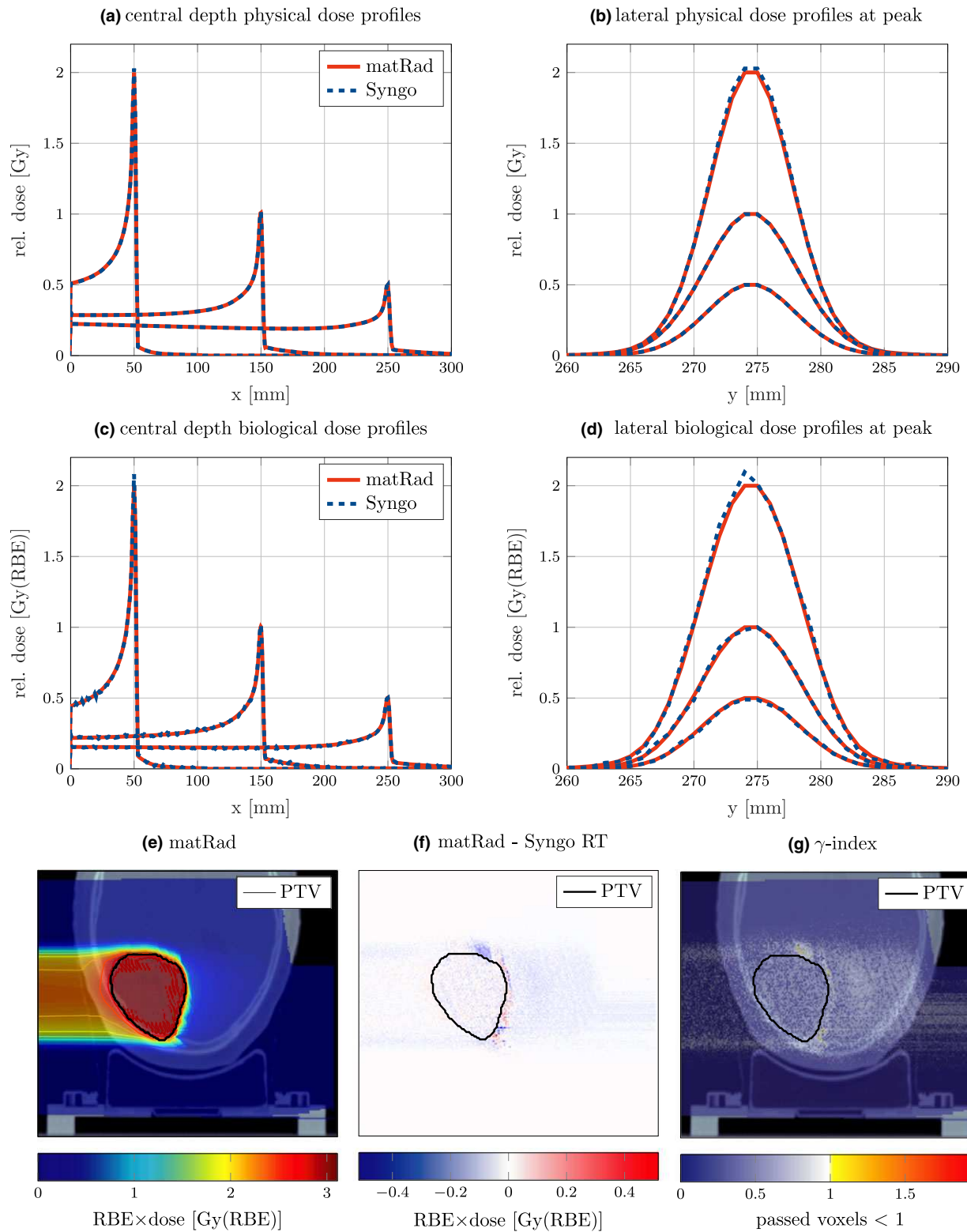


FIG. 4. Comparison of the carbon ion dose calculation engine of Syngo RT and matRad. Dashed lines in (a)–(d) indicate dose values calculated by Syngo RT and solid lines refer to dose values based on matRad. Three single energy carbon ion beams with peak positions at 5 mm, 15 cm, and 25 mm are evaluated considering physical (a and b) and RBE weighted dose (c and d) separately. (a) and (c) show central profiles of each beam as a function of depth whereas (b) and (d) illustrate lateral dose profile at the peak position. Profiles have been rescaled to maxima at 2, 1, and 0.5 for better separation of the data. Global  $\gamma$ -analysis pass rates (dta = 2 mm,  $\Delta d$  = 2%) are for the RBE weighted dose and (physical dose) 99.46%, 99.93%, and 99.95% (99.81%, 99.99%, and 99.99%), respectively. (e)–(g) Transversal slices of a carbon ion treatment plan for a cranial case using one beam with gantry angle 270° and couch angle 0°. (e) CT data superimposed with transparent dose colorwash and isodose lines calculated with matRad. The absolute difference between matRad and Syngo RT planning is shown in (f). The result of the  $\gamma$ -analysis is illustrated in (g) showing a pass rate for (dta = 2 mm,  $\Delta d$  = 2%) of 99.67%.

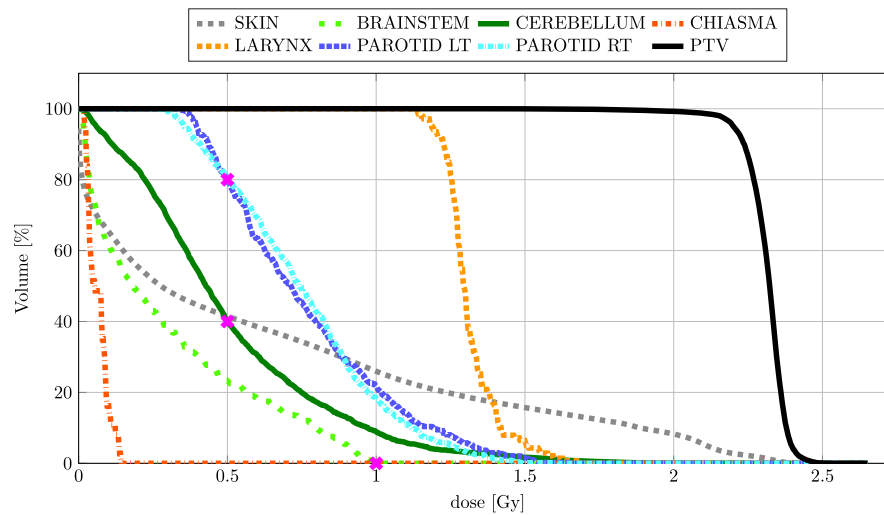


FIG. 5. Resulting dose volume histogram (DVH) of an inversely optimized intensity-modulated photon treatment plan using seven linearly spaced beam directions based on the open-source head and neck patient case. Given constraints are shown by purple crosses.

produced by different particle species. This procedure is executed for each dose calculation point individually to assess the RBE in a mixed radiation field. Even 1000 Monte Carlo loops yield to considerable uncertainties in a single dose calculation point as can be seen in Fig. 4(c) by the dashed line. The number of loops would have to be further increased to avoid local fluctuations. On the contrary, matRad facilitates RBE calculations relying on base data stemming from a rapid analytical extension presented in Ref. 19. Using this approach limits matRad to calculate RBE-weighted fraction doses smaller than 10 Gy(RBE).

The results of the single energy carbon ion beams are illustrated in Figs. 4(a)–4(d). The statistical noise stemming from the Monte Carlo simulation can be seen in the dashed curves in Figs. 4(c) and 4(d). Profiles were scaled for visualization to exhibit maxima at 2, 1 and 0.5 Gy (RBE). Central profiles illustrated in 4a, 4c and lateral profiles at the peak position shown in 4b, 4d are in good agreement. Considering the physical dose, we obtain  $\gamma$ -analysis pass rates of 99.81%, 99.99%, and 99.99% using a distance to agreement of 2 mm and a dose difference criteria of 2%. Complementary, the global  $\gamma$ -analysis pass rates for the RBE-weighted dose volumes are 99.46%, 99.93%, and 99.95% whereas 99% of voxels receiving RBE-weighted dose depict a deviation of less than 0.49%, 0.21%, and 0.19%, respectively.

The comparison between matRad and Syngo RT Planning utilizing carbon ions for a realistic patient case is depicted in Figs. 4(e)–4(g). The results show that differences occur mainly at the distal edge of the PTV and in the fragmentation tail, but 90% of voxels receiving dose do not exceed a deviation of 1% with reference to the prescribed dose of 3 Gy (RBE). The  $\gamma$ -analysis results in a global pass rate of 99.67%.

Apart from the statistical noise, differences between the carbon ion dose distributions calculated with matRad and Syngo RT can be explained by the usage of different algorithms to determine the three-dimensional RBE. Also discretization effects of the underlying ray tracing causing rays

to cross slightly different voxels may be responsible for dose differences at the abrupt dose fall-off behind the Bragg peak.

### 3.B. Optimization

#### 3.B.1. Evaluation of objective and constraint functions

To verify the mathematical consistency of all implemented objective and constraint functions together with their partial derivatives, analytical gradients are compared against numerical gradients. To test a correct communication with IPOPT, the head and neck patient case of the CORT dataset is optimized in matRad using 10 optimization criteria. Besides, a squared dose deviation objective with a reference dose of 2.33 Gy, the 80% volume of the left and right parotid gland is constrained to doses below 0.50 Gy, the 40% volume of the cerebellum is constrained to doses below 0.50 Gy, and the maximum dose to the brain stem is constrained below 1.00 Gy. The treatment plan uses seven beams with equally spaced coplanar beam orientations. As depicted in the dose volume histogram (DVH) in Fig. 5, all constraints are obeyed by the final result of the optimization.

#### 3.B.2. Runtimes

To investigate the performance of the dose calculation and fluence optimization in matRad, multiple treatment planning scenarios based on the open-source patients with varying problem size are defined. Each of it is exercised three times. The resulting average calculation times are shown in Table II together with plan specific parameters depicting the problem size. Default optimization parameters, predefined in the *csf* variable of the patient data, were used in combination with default convergence criteria provided by the IPOPT options file. Depending on the scenario, we used different lateral cut-offs for dose calculation to lower the number of dose

TABLE II. Computational efficiency of matRad for selected treatment planning scenarios using a CT and dose grid resolution of  $0.3 \text{ cm}^3$ . Given are average run-times on a machine with the following specifications: Intel Core i7 860, 2.8 GHz, 16 GB RAM @ 1333 MHz. Columns from left to right illustrate the radiation modality, dose calculation setting, number of bixels/pencil beams, total number of dose influence elements, storage size of dose influence data, elapsed time for dose calculation, number of optimization iterations, elapsed time for optimization, and memory throughput rate per second. The setting column depicts in the case of photons the lateral cutoff with either performing or omitting  $D_{ij}$  importance sampling. For charged particles, the lateral cutoff is determined on runtime to account for a given percentage of integral lateral dose using either the single Gaussian (SG) or double Gaussian (DG) beam model

Modality	Setting	#beams	#bixel	$D_{ij}$ elem. [1e6]	$D_{ij}$ size [GB]	$t_{dose}$ [s]	#iter.	$t_{opt}$ [s]	Throughput [GBs <sup>-1</sup> ]
Photons	82 mm $D_{ij}$ samp.	4	2608	172	2.75	295	145	82	4.89
Photons	40 mm no samp.	4	2608	99	1.59	101	143	44	5.17
Photons	82 mm $D_{ij}$ samp.	8	3877	426	6.81	741	51	140	4.99
Photons	40 mm no samp.	8	3877	236	3.77	226	51	66	3.77
Photons	40 mm $D_{ij}$ samp.	72	13597	567	9.07	853	147	407	6.69
Protons	99.75% SG	1	7797	19	0.29	22	123	41	1.78
Protons	99.75% DG	1	5955	87	1.38	46	171	109	4.47
Protons	99.75% SG	3	28097	56	0.89	68	67	187	4.90
Protons	99.75% DG	3	24137	269	4.30	160	262	330	6.85
Protons	99.75% SG	2	45574	116	1.86	97	218	137	6.13
Protons	99.75% DG	2	27683	520	8.33	299	197	486	6.90
Carbon	99.75% SG	1	11780	160	2.55	67	72	92	3.49
Carbon	99.75% DG	1	9963	537	8.61	203	79	225	5.14
Carbon	99.75% SG	3	42810	411	6.68	310	117	193	6.68
Carbon	99.75% DG	3	31205	756	12.1	560	107	365	6.17
Carbon	99.75% SG	2	24612	336	5.88	137	177	273	5.88
Carbon	99.50% DG	2	16889	855	17.94	472	134	521	5.93

influence elements. Dose influence data are only taken into account if a dose calculation point depicts a smaller geometrical distance to the central ray of the current bixel/pencil beam than the given lateral cutoff. Moreover, dose calculation and optimization times are given for single and double Gaussian lateral beam model.

We observe an average memory throughput rate of  $5.2 \text{ GB}_s^{-1}$  during dose optimization. Dose calculation times lie in the range of a reference computer processing unit (CPU)-based implementation using C++ code.<sup>33</sup> Although using highly vectorized code and reducing the number of for loops to a minimum, there is inevitably a trade-off between speed and flexibility when comparing run times of an interpreted programming languages to highly optimized implementations.<sup>11</sup> Total run times for photons and (charged particles including biological optimization for carbon ions) are in the range of 145–1260 s (63–993 s) for dose calculation and fluence optimization. The memory consumption lies between 1.59–9.07 GB (0.29–17.94 GB) at a voxel resolution of  $0.3 \text{ cm}^3$ .

#### 4. DISCUSSION

This paper introduces the functionalities of the open-source cross-platform dose calculation and optimization toolkit matRad and describes its evaluation process. matRad is the first open-source treatment planning system that supports three different radiation modalities, namely photons, scanned protons, and scanned carbon ions. Unlike other open-source software projects in radiation therapy,<sup>5–9</sup> matRad

has a clear focus on dose calculation and fluence optimization. Therefore, matRad uses well-established algorithms and provides efficient implementations even though it relies on an intuitive interpreter programming language.

We choose the proprietary scientific programming environment Matlab because it encourages on the one hand efficient algorithm prototyping and ensures on the other hand reasonable run times. Additionally Matlab's visualization and debugging capabilities permit quick data and code exploration. Although Matlab is not freely available for download, it is ubiquitous in the medical physics community and at universities. Also, matRad can be used in combination with the free programming environment Octave instead of Matlab at no charge. However, using Octave does not support the graphical user interface. Mainly for educational purposes, we also provide a Windows standalone application that does not require a full Matlab installation. We actively tested maRad against Matlab versions  $\leq 8.3$  (R2014a) on Windows, Mac OS, and Linux. Nevertheless, the functionality of matRad maybe compromised when using earlier Matlab versions.

Versatile and efficient dose calculation and optimization algorithms are essential tools for radiation therapy and are likely to get more computationally demanding in the future for more complex tasks in relation to 4D and robust treatment planning. Given that possibilities to increase the performance of matRad are limited, high level programming language implementations come unavoidable into place for certain use cases. Highly optimized code written in abstract programming languages implemented in closed-source represents one

end of the spectrum, while open-source programs using an interpreter programming language represent the other end of the spectrum. Although both approaches have different use cases, both are justified and complement each other.

matRad is under constant development in our department. For the future, we consider to decouple the dose grid from the CT grid so that dose can be calculated on a different resolution than the CT used for ray tracing. Also, we want to implement an interface to CERR and a unit testing environment to maintain high code quality within a growing matRad project. Currently, we focus on the incorporation of robust treatment planning methods into matRad and we are working towards a release including functionality for single-field-uniform-dose, worst case,<sup>34</sup> probabilistic,<sup>35,36</sup> coverage-based optimization,<sup>37</sup> and variable RBE models for protons.<sup>38</sup> Ideally, this publication also encourages external groups to contribute to matRad. We have set up a suited infrastructure with an online versioning system and a license that supports collaboration. matRad is already used for research at Klinikum Rechts der Isar, Munich, Germany, University of Zürich, Switzerland and at Carleton University, Ottawa, Canada. Other international research groups are currently considering matRad.

## 5. CONCLUSION

matRad is an open-source toolkit for three-dimensional intensity-modulated radiation treatment planning entirely written in Matlab. It supports photons, scanned protons, and scanned carbon ions — for the latter, including a three-dimensional variable relative biological effectiveness model. matRad comprises the source code itself, physical as well as biological beam base data, and patient data. Comparing matRad dose calculations against clinically approved treatment planning systems, we observe good agreement with global  $\gamma$ -analysis pass rates  $\geq 99.67\%$  (dta = 2 mm,  $\Delta d = 2\%$ ) for all radiation modalities. Dose calculation and optimization times for realistic patient cases is a matter of view minutes. All modules of matRad are available for the medical physics community to download for free. matRad has direct practical relevance and encourages an application for educational and research purposes.

## ACKNOWLEDGMENTS

The authors acknowledge the support of a continuously growing matRad community on GitHub. Furthermore, we thank Peter Ziegenhein, Martin Siggel, Thomas Tessonier, Aluisio Castro, Oliver Schrenk, Verena Böswald, and Cindy Herrmann for their contributions to the matRad project. Financial support from the German Research Foundation, Grant No. BA 2279/3-1, is gratefully acknowledged.

## CONFLICTS OF INTEREST

The authors have no relevant conflicts of interest to disclose.

<sup>a)</sup>Author to whom correspondence should be addressed. Electronic mail: h.wieser@dkfz-heidelberg.de.

## REFERENCES

- Ince DC, Hatton L, Graham-Cumming J. The case for open computer programs. *Nature*. 2012;482:485–488.
- Krämer M, Jäkel O, Haberer T, Kraft G, Schardt D, Weber U. Treatment planning for heavy-ion radiotherapy: physical beam model and dose optimization *Phys Med Biol*. 2000;45:3299–3317.
- Breedveld S, Storchi PRM, Voet PWJ, Heijmen BJM. iCycle: integrated, multicriterial beam angle, and profile optimization for generation of coplanar and noncoplanar IMRT plans. *Med Phys*. 2012; 39:951–963.
- Kamerling CP, Ziegenhein P, Heinrich H, Oelfke U. A 3D isodose manipulation tool for interactive dose shaping. *J Phys*. 2014;489: 012052.
- Sánchez-Parcerisa D, Kondrla M, Shaindlin A, Carabe A. FoCa: a modular treatment planning system for proton radiotherapy with research and educational purposes. *Phys Med Biol*. 2014;59:7341–7360.
- Tewell MA, Adams R. The plunc 3d treatment planning system: a dynamic alternative to commercially available systems. *Med Dosim*. 2004;29:134–138.
- Deasy JO, Blanco AI, Clark VH. CERR: a computational environment for radiotherapy research. *Med Phys*. 2003;30:979–985.
- Pinter C, Lasso A, Wang A, Jaffray D, Fichtinger G. SlicerRT: radiation therapy research toolkit for 3D Slicer. *Med Phys*. 2012;39:6332–6338.
- Desplanques M, Wang K, Phillips J, Gueorguiev G, Baroni G, Sharp G. TH-A-19A-01: An Open Source Software for Proton Treatment Planning in Heterogeneous Medium. *Med Phys*. 2014;41:533–533.
- MATLAB. Version 8.5 (R2015a). The MathWorks Inc.; 2015.
- Siggel M, Ziegenhein P, Nill S, Oelfke U. Boosting runtime-performance of photon pencil beam algorithms for radiotherapy treatment planning. *Phys Med*. 2012;28:273–280.
- Bortfeld T, Schlegel W, Rhein B. Decomposition of pencil beam kernels for fast dose calculations in three-dimensional treatment planning. *Med Phys*. 1993;20:311–318.
- Bortfeld T. An analytical approximation of the Bragg curve for therapeutic proton beams. *Med Phys*. 1997;24:2024.
- Gottschalk B, Koehler AM, Schneider RJ, Sisterson JM, Wagner MS. Multiple Coulomb scattering of 160 MeV protons. *Nuclear Instrum Methods Phys Res B*. 1993;74:467–490.
- Safai S, Bula C, Meer D, Pedroni E. Improving the precision and performance of proton pencil beam scanning. *Transl Cancer Res*. 2012;1:196–206.
- Parodi K, Mairani A, Brons S, et al. Monte Carlo simulations to support start-up and treatment planning of scanned proton and carbon ion therapy at a synchrotron-based facility. *Phys Med Biol*. 2012;57:3759–3784.
- Kellerer A, Rossi H. A Generalized Formulation of Dual Radiation Action. *Radiat Res*. 1978;75:471.
- Elsässer T, Weyrather WK, Friedrich T, et al. Quantification of the relative biological effectiveness for ion beam radiotherapy: direct experimental comparison of proton and carbon ion beams and a novel approach for treatment planning. *Int J Radiat Oncol Biol Phys*. 2010;78:1177–1183.
- Krämer M, Scholz M. Rapid calculation of biological effects in ion radiotherapy. *Phys Med Biol*. 2006;51:1959–1970.
- Zaider M, Rossi H. The synergistic effects of different radiations. *Radiat Res*. 1980;83:732–739.
- Craft D, Bangert M, Long T, Papp D, Unkelbach J. Shared data for intensity modulated radiation therapy (IMRT) optimization research: the CORT dataset. *Giga Sci*. 2014;3:37.
- Nill S. Development and application of a multimodality inverse treatment planning system (in English). *Med Phys*. 2002;29:258.
- Siddon RL. Fast calculation of the exact radiological path for a three-dimensional CT array. *Med Phys*. 1984;12:252–255.
- Thieke C, Nill S, Oelfke U, Bortfeld T. Acceleration of intensity-modulated radiotherapy dose calculation by importance sampling of the calculation matrices. *Med Phys*. 2002;29:676–681.

25. Hong L, Goitein M, Bucciolini M, et al. A pencil beam algorithm for proton dose calculations. *Phys Med Biol*. 1996;41:1305–1330.
26. Wächter A, Biegler LT. On the implementation of an interior-point filter line-search algorithm for large-scale nonlinear programming. *Math Program*. 2006;106:25–57.
27. Xia P, Verhey LJ. Multileaf collimator leaf sequencing algorithm for intensity modulated beams with multiple static segments. *Med Phys*. 1998;25:1424–1434.
28. Engel K. A new algorithm for optimal multileaf collimator field segmentation. *Discrete Appl Math*. 2005;152:35–51.
29. Wild E, Bangert M, Nill S, Oelfke U. Noncoplanar VMAT for nasopharyngeal tumors: plan quality versus treatment time. *Med Phys*. 2015;42:2157–2168.
30. Wilkens JJ, Oelfke U. Fast multifield optimization of the biological effect in ion therapy. *Phys Med Biol*. 2006;51:3127–3140.
31. Krämer M, Scholz M. Treatment planning for heavy-ion radiotherapy: calculation and optimization of biologically effective dose. *Phys Med Biol*. 2000;45:3319–3330.
32. Low D, Harms W, Mutic S, Purdy JA. A technique for the quantitative evaluation of dose distributions. *Med Phys*. 1998;25:656.
33. Gu X, Cho D, Men C, Pan H, Majumdar A, Jiang SB. GPU-based ultrafast dose calculation using a finite size pencil beam model. *Phys Med Biol*. 2009;54:6287.
34. Fredriksson A, Bokrantz R. A critical evaluation of worst case optimization methods for robust intensity-modulated proton therapy planning. *Med Phys*. 2014;41:081701.
35. Bangert M, Hennig P, Oelfke U. Analytical probabilistic modeling for radiation therapy treatment planning. *Phys Med Biol*. 2013;58:5401–5419.
36. Unkelbach J, Bortfeld T, Martin BC, Soukup M. Reducing the sensitivity of IMPT treatment plans to setup errors and range uncertainties via probabilistic treatment planning. *Med Phys*. 2009;36:149–163.
37. Gordon JJ, Sayah N, Weiss E, Siebers JV. Coverage optimized planning: probabilistic treatment planning based on dose coverage histogram criteria. *Med Phys*. 2010;37:550–563.
38. McNamara AL, Schuemann J, Paganetti H. A phenomenological relative biological effectiveness (RBE) model for proton therapy based on all published in vitro cell survival data. *Phys Med Biol*. 2015;60:8399–8416.
39. Alfredo R, Siochi C. Minimizing static intensity modulation delivery time using an intensity solid paradigm. *Int J Radiat Oncol Biol Phys*. 1999;43:671–680.